American Mineralogist, Volume 76, pages 1811–1823, 1991

Structural defects in synthetic tremolitic amphiboles

Jung Ho Ahn*
Department of Geology, Arizona State University, Tempe, Arizona 85287-1404, U.S.A.
Moonsup Cho**
Department of Geology, Stanford University, Stanford, California 94305-2115, U.S.A.
David M. Jenkins
Department of Geological Sciences and Environmental Studies, State University of New York at Binghamton, Binghamton, New York 13901, U.S.A.
Peter R. Buseck
Departments of Geology and Chemistry, Arizona State University, Tempe, Arizona 85287-1404, U.S.A.

Abstract

Synthetic hydroxyl tremolite, fluor-tremolite, and magnesio-hornblende together with two natural tremolite samples were investigated using high-resolution transmission electron microscopy (HRTEM). Chain-width defects are widespread in both hydroxyl tremolite and magnesio-hornblende synthesized at pressures and temperatures ranging from 2 to 10 kbar and 701 to 853 °C. In contrast, fluorine tremolite synthesized at 2.13 kbar and 1000 °C is virtually free of such defects, similar to natural tremolite that is completely ordered. The degree of structural ordering described in terms of the $A'(2)$ value (= width ratio of total double-chain fringes vs. entire measured crystal in TEM images) ranges from 0.8 for low-temperature hydroxyl tremolite to 1.0 for fluorine tremolite. Synthetic amphiboles containing many structural defects [low $A'(2)$ values] tend to be more elongated than those that are better ordered. Triple-chain structures predominate among intergrown pyriboles and occur in slabs of widths equivalent to 3–30 single chains. Their abundance is inversely proportional to that of double-chain structures, suggesting that the triple-chain silicate may be an important precursor to calcic amphibole during synthesis. Single-chain structures occur in amphibole crystals as both isolated units and pyroxene slabs ranging up to 0.1 μm in width along the **b** axis. Pyriboles with chain widths greater than seven subchains are absent in all of the observed synthetic calcic amphiboles.

Temperature is apparently the most critical experimental variable affecting the number of chain-width defects in synthetic amphiboles. In addition, the seeding technique using defect-free natural tremolite greatly increases the structural order in synthetic amphibole. The widespread intergrowth of chain silicates with various widths probably contributes to the lower thermal stability of synthetic vs. natural tremolite because the intergrown wide-chain pyriboles will affect the composition (greater Mg and OH content) and increase the structural disorder of synthetic tremolitic amphiboles.

Introduction

Syntheses of tremolite have been of great interest because of its relatively simple chemistry and importance in many phase equilibrium studies (e.g., Boyd, 1959; Jenkins, 1987). However, synthetic and natural tremolite appear to show significant differences in thermal stability. Skippen and McKinstry (1985) compared the reaction tremolite + forsterite = 2 diopside + 5 enstatite + H_2O using natural and synthetic tremolite and found that the reaction temperature at 1 kbar using synthetic tremolite is about 133 °C lower than that using natural end-member tremolite. Jenkins and Clare (1990) investigated the reaction tremolite = 2 diopside + 3 enstatite + quartz + H_2O at pressures of 1.5–7 kbar and found that the upper thermal stability of synthetic tremolite is about 40 °C lower than that of natural tremolite.

Such differences in thermal stabilities can result from the dissimilarity in chemistry or structural state or both between synthetic and natural tremolite. Jenkins and Clare (1990) suggested that the F content of natural tremolite is sufficient to account for the difference in the thermal stabilities. There has not been an investigation of the structural defects in the tremolite used in either the study of Skippen and McKinstry (1985) or that of Jenkins and Clare (1990) in order to evaluate the contribution of de-

* Present address: Korea Ocean Research and Development Institute, Ansan P.O. Box 29, Seoul 425-600, Korea.
** Present address: Department of Geological Sciences, Seoul National University, Seoul 151-742, Korea.

0003–004X/91/1112–1811$02.00

TABLE 1. Experimental data for synthesis of tremolite and magnesio-hornblende

Experiment no.*	P (kbar)	T (°C)	Duration (h)	wt% H_2O	Starting materials	Crystalline products**
Tr1-21	2.0 ± 0.1	740 ± 5	188	30	oxide mixture of composition $Ca_2Mg_5Si_8O_{22}(OH)_2$	tc + cpx + trm + qtz
		806 ± 8	214	17		trm + cpx + qtz(?)
Tr5-18	5.88 ± 0.06	853 ± 8	192	17	oxide mixture of composition $Ca_{1.8}Mg_{5.2}Si_8O_{22}(OH)_2$	trm + qtz
Tr2	2.0 ± 0.05	701 ± 6	1152	14	oxide mixture of composition $Ca_2Mg_5Si_8O_{22}(OH)_2$ + 0.5 SiO_2	trm + qtz + cpx + tc
Tr6	2.0 ± 0.05	750 ± 5	648	8	same oxide mixtures as Tr2, but seeded with natural tremolite‡	trm + qtz + cpx(?)
Tr19-1	2.13 ± 0.05	1000 ± 15	192	0	mixture of $CaCO_3$ + CaF_2 + MgO + SiO_2	F-trm + qtz + fluorite(?)
Hb19	10.0 ± 0.05	751 ± 10	141	9	gel of composition $Ca_2Mg_4Al_2Si_7O_{22}(OH)_2$	hb + anorthite

* Tr1-21, Tr5-18, and Tr19-1 were synthesized by D.M. Jenkins at SUNY–Binghamton, and Tr2, Tr6, and Hb19 were synthesized by M. Cho at UCLA.

** Experimental products were characterized by powder X-ray diffraction. Abbreviations: cpx, clinopyroxene; tc, talc; trm, tremolite; F-trm, fluor-tremolite; qtz, quartz; and hb, magnesio-hornblende.

† Tr1-21 was synthesized in two steps.

‡ The composition of natural seed tremolite (SUMC5122) is $Na_{0.07}K_{0.01}Ca_{1.96}Mg_{4.93}Fe_{0.02}Al_{0.01}Si_{8.01}O_{22}(OH)_2$ (Cho and Ernst, 1991).

fects to the thermal stabilities of amphiboles. The apparent discrepancy between these further suggests that the structural perfection of synthetic tremolite may depend significantly on experimental techniques and conditions. It is therefore important to characterize synthetic amphiboles with transmission electron microscopy (TEM) before the experimental data are applied to natural analogues.

Previous TEM studies of synthetic amphiboles are limited in number but show that most synthetic amphiboles contain defects with wide-chain pyribole structures. Veblen et al. (1977) found that all of the synthetic anthophyllite samples they examined are structurally disordered, in some cases consisting of intimate mixtures of chains of many widths. Chernosky and Autio (1979) reported that synthetic anthophyllite studied with TEM by Veblen contains approximately 5 vol% triple-chain structures. Maresch and Czank (1983, 1988) found numerous intergrowths of wide-chain biopyriboles in synthetic manganese magnesium amphiboles.

To quantify the structural disorder in amphiboles, Maresch and Czank (1988) defined an "A value." It is the ratio of the width of regions of ideal, undisturbed amphibole to the width of the amphibole crystal as a whole. At least one unit cell, equivalent to two double-chain fringes (four individual fringes) in a high-resolution transmission electron microscopy (HRTEM) image of orthoamphibole, is required for "undisturbed" amphibole. The A values of manganese magnesium amphiboles synthesized by Maresch and Czank (1988) vary from 0.23 to 0.90. Futhermore, they found an A value of ~0.70 for a tremolite sample synthesized at 700 °C and 5 kbar for 936 h. In contrast, Skogby and Ferrow (1989) reported that Fe-bearing tremolite synthesized from oxide mixtures with Fe/Mg ratios between 0.07 and 0.14 contains intergrown wide-chain structures estimated to be significantly less abundant than a few volume percent. These TEM results raise the possibility that structural defects are also widespread in synthetic tremolitic amphiboles. However, the extent and type of chain multiplicity faulting in synthetic tremolite are still unknown because detailed TEM study has not been done.

Using HRTEM, we investigated the structural defects of synthetic tremolite samples that were prepared in two different laboratories. We also examined synthetic fluorine tremolite and magnesio-hornblende that were synthesized at relatively high temperature and pressure, respectively. The goals of this study were to investigate the degree of structural perfection of these synthetic amphiboles and to compare the effects of various experimental variables on the structural state of synthetic amphiboles. Finally, we wished to understand the reaction processes involved in the crystallization of double-chain structures.

EXPERIMENTAL METHODS

Synthesis techniques

OH-bearing amphiboles synthesized at SUNY–Binghamton (Tr1-21, Tr5-18) were made by the hydrothermal treatment of mixtures of reagent grade $CaCO_3$, MgO, and SiO_2 according to the bulk compositions and conditions given in Table 1. Both starting mixtures were decarbonated by heating for 1 min to approximately 900 °C in air prior to being sealed in Pt capsules with 17 or 30 wt% H_2O. These experiments were performed in cold-seal vessels using H_2O as the pressurizing medium (Jenkins, 1987). Tr1-21 had a bulk composition corresponding to ideal tremolite, whereas Tr5-18 had a Mg-enriched bulk composition. It is believed that both starting mixtures produced virtually the same Mg-enriched tremolite, as reflected in the phase assemblages obtained (Table 1; Jenkins, 1987). Sample Tr1-21 was prepared in two steps. It was first prepared at 740 °C, which produced a talc- and

diopside-rich assemblage, and then heated at 806 °C, which removed talc [confirmed by the absence of the distinctive 002 reflection with X-ray diffraction (XRD)] and greatly improved the yield of tremolitic amphibole.

Fluorine tremolite was synthesized from a mixture of $CaCO_3$, CaF_2, MgO, and SiO_2 without water using an internally heated vessel with Ar as the pressure medium (Jenkins, 1987). The starting mixture was dried at about 600 °C immediately prior to sealing in a Ag-Pd capsule. This temperature was chosen to be high enough to ensure that no H_2O was introduced into the capsule, yet low enough to prevent the decarbonation of $CaCO_3$. Although not firmly established, the presence of CO_2 may be sufficiently conducive to the transport of cations to facilitate growth of reasonably large crystals. At the conclusion of the experiment, the capsule was pierced and weighed immediately to check that all of the CO_2 had been driven into the ambient fluid. The observed weight loss of 5.2 wt% is essentially identical to the loss of 5.1 wt% that was anticipated from CO_2 liberation. Examination of the experimental products with the petrographic microscope showed euhedral crystals that were markedly larger and more equant (about 30 μm wide by 50 μm long, on the average) than the synthetic hydroxyl tremolite crystals (typically 2 by 10 μm).

Tr2 and Tr6 were synthesized at UCLA using conventional cold-seal pressure vessels. Temperatures of the experiments were monitored by Inconel-sheathed chromel-alumel thermocouples placed in external thermocouple wells. Uncertainties in temperatures (Table 1) result from a combination of the thermal gradient over the capsule length, uncertainties in thermocouple calibration, and day-to-day fluctuations in recorded temperature. Estimated uncertainties of pressure are ± 50 bars.

The starting material for Tr2 and Tr6 was an oxide mixture made from reagent-grade $CaCO_3$, hydrous $MgCO_3$, and silicic acid. Excess silica from the tremolite composition was attained in the mix according to a stoichiometric proportion of $2CaO \cdot 5MgO \cdot 8.5SiO_2$ in order to saturate the ambient fluid in SiO_2 (Jenkins, 1987). In addition, the starting mix of Tr6 was seeded with 7 wt% natural tremolite (SUMC 5122) to enhance the yield of tremolite.

Hb19 was synthesized at UCLA using a conventional piston-cylinder apparatus. A 2.54-cm diameter furnace assembly consisting of NaCl, pyrex, graphite, BN, and MgO was used, and no pressure correction for friction was required. Estimated uncertainties in P and T measurements are ± 500 bars and ± 10 °C, respectively. The starting material for Hb19 was a gel with the stoichiometric proportion of $2CaO \cdot 4MgO \cdot Al_2O_3 \cdot 7SiO_2$. Further details on experimental procedures are available in Cho and Ernst (1991).

Hydroxyl tremolite and magnesio-hornblende synthesized at UCLA were produced by sealing a portion of the appropriate starting mix in Au capsules with 8–14 wt% H_2O (Table 1). At the conclusion of the experiments, each capsule was checked for leakage by weighing, puncturing, and drying at 130 °C. XRD indicates that the yield of amphibole in Tr6 and Hb19 is greater than 90 wt% (Table 1). In contrast, Tr2 contains a significant amount of clinopyroxene and talc as metastable precursors to tremolite.

Transmission electron microscopy

All experimental products except Hb19 were disaggregated using an ultrasonic vibrator in order to minimize the mechanical breakage of individual crystals. Because of the compact nature of the product, Hb19 was ground with a mortar and pestle to reduce the size of the crystalline aggregate prior to TEM observation. Natural tremolite was also ground. Disaggregated crystals were dispersed in acetone and mounted on holey-carbon substrates. Portions of the samples were embedded in epoxy resin, and ion-milled specimens were prepared to investigate the cross sections of elongated crystals.

Specimens were examined at 400 kV with a JEOL JEM-4000EX transmission electron microscope that has a top-entry, double-tilting sample holder that is capable of $\pm 30°$ tilts at 0.5 mm above the standard specimen height. The microscope has a structure resolution limit of 1.7 Å and a spherical aberration coefficient (C_s) of 1.0 mm. A 40-μm objective aperture and a 150-μm condenser aperture were used for HRTEM imaging; all TEM images reported here are bright-field images.

HRTEM images were interpreted based on the results of Veblen et al. (1977) and Akai (1982). Image calculations by Akai (1982) showed that **a**-axis images of triple-chain structure slabs exhibit two rows of white spots at the underfocused condition. Experimental **a**-axis images by Veblen et al. (1977) also indicated that widths of chain structures are defined by strong dark fringes at underfocused conditions.

TEM RESULTS

Crystal morphology

Synthetic tremolite amphiboles. All hydroxyl tremolite consists of slender prismatic crystals elongated parallel to the **c** axis (Figs. 1a–1d). Typical synthetic tremolite crystals are 1–2 μm long and less than 0.3 μm wide, but their aspect ratios vary among different experimental products. The sizes of crystals as observed using TEM are smaller than those determined by optical microscopy. This apparent discrepancy is attributed to our sample preparation method using the dispersion of disaggregated crystals. Tr2 is most elongate, with aspect ratios ranging up to ~50. Fluorine tremolite and magnesio-hornblende generally appear as stubby prisms (Figs. 1e and 1f) rather than the elongated crystals that are characteristic of hydroxyl tremolite. Crystals of fluorine tremolite are bigger than other synthetic amphiboles, and some also show distinct crystal habits (Fig. 1e). As a result of mechanical grinding, the sizes of magnesio-hornblende crystals vary

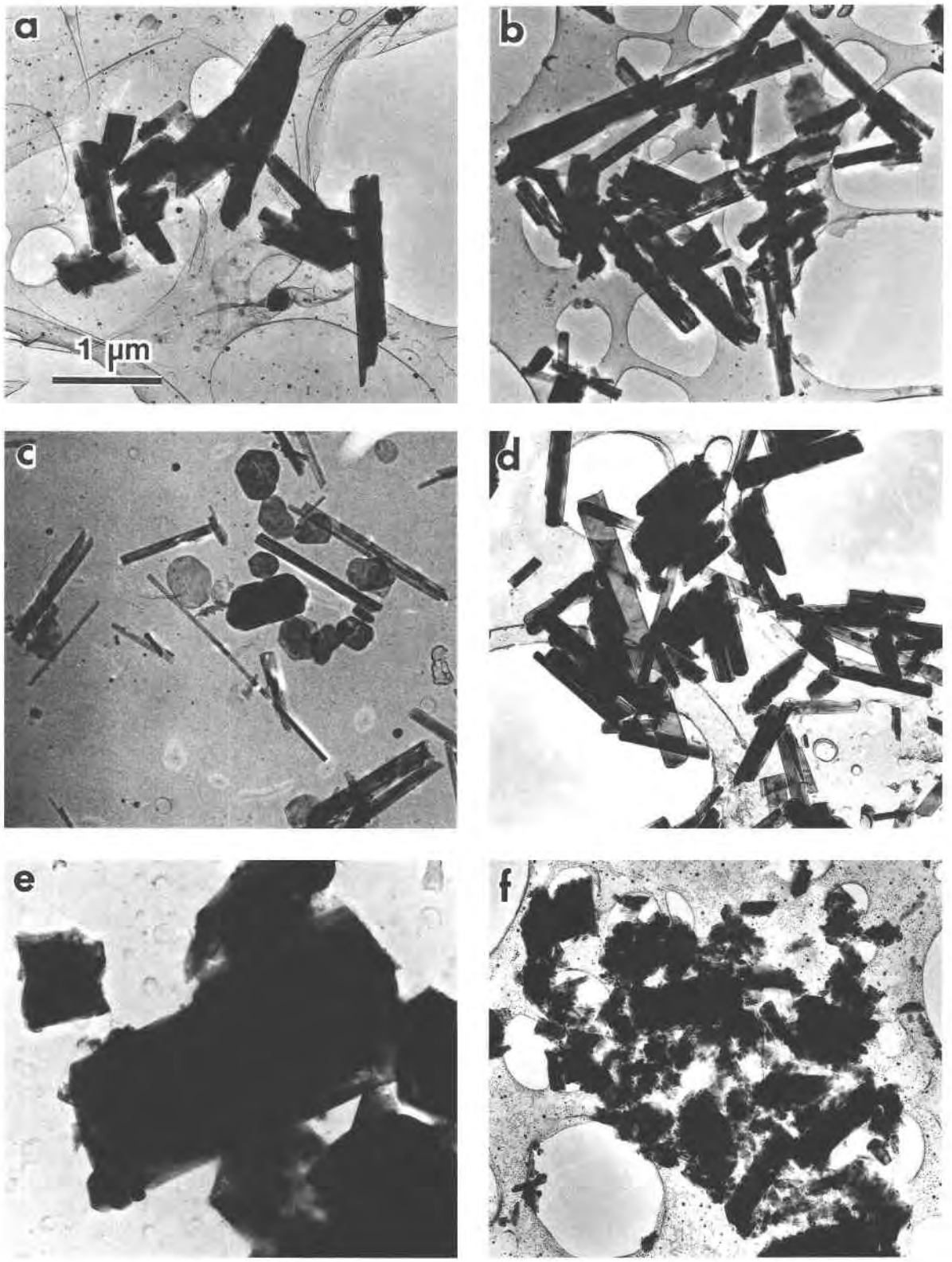

Fig. 1. Low-magnification TEM images of synthetic tremolitic amphiboles: (**a**) Tr1-21, (**b**) Tr5-18, (**c**) Tr2, (**d**) Tr6, (**e**) Tr19-1, and (**f**) Hb19. Talc occurs in Tr2, **c**, as pseudohexagonal plates. All images are at the same magnification, and a 1-μm scale bar is shown in **a**.

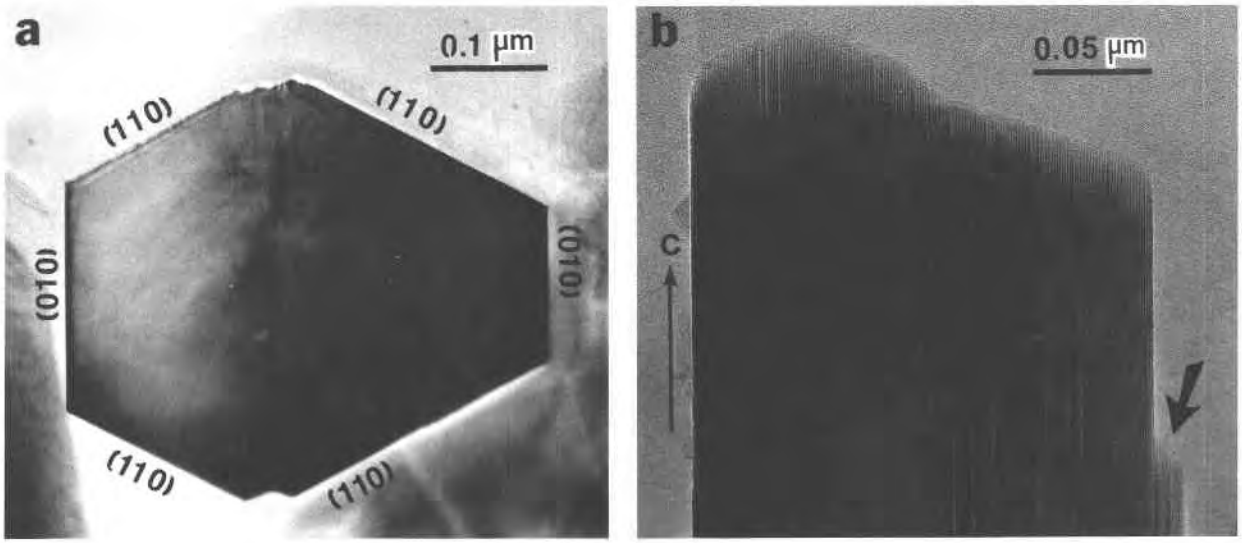

Fig. 2. (**a**) TEM image of a cross section of a tremolite prism in Tr5-18. The crystal has an approximately hexagonal shape defined by {110} and {010}. This image was obtained from an ion-milled sample. (**b**) TEM image of the curved basal surface of a tremolite crystal (Tr5-18). Many structural defects are evident, even at this relatively low magnification. The arrow indicates a growth ledge.

significantly compared with other amphiboles (Fig. 1f). Most magnesio-hornblende crystals observed by TEM are, therefore, cleavage fragments.

Cross-section images of hydroxyl tremolite show that {010} and {110} faces develop well, in contrast to the absence of well-defined {100} faces (Fig. 2a). Growth ledges along the **c** axis are commonly observed in elongate crystals and are attributed to rapid growth in the direction of the **c** axis. The basal surface commonly is rounded or curved as a result of the lack of a well-defined (001) face (Fig. 2b). These phenomena, together with the elongate shape of synthetic amphibole crystals, are consistent with the Bravais law that growth is fastest in the direction with the smallest lattice spacing.

Natural tremolite. We also examined two natural tremolite samples, Tr12 and SUMC5122, using HRTEM. Tr12 was utilized for dissolution and regrowth experiments by Jenkins (1987), and SUMC5122 was used as seed crystals in the synthesis of Tr6 (Table 1). Selected-area electron diffraction (SAED) patterns from both natural tremolite samples (Fig. 3) do not show any streaking, in contrast to synthetic tremolite (see below), indicating that natural tremolite is free of chain-width disorder. The absence of other intergrown pyriboles in natural tremolite was con-

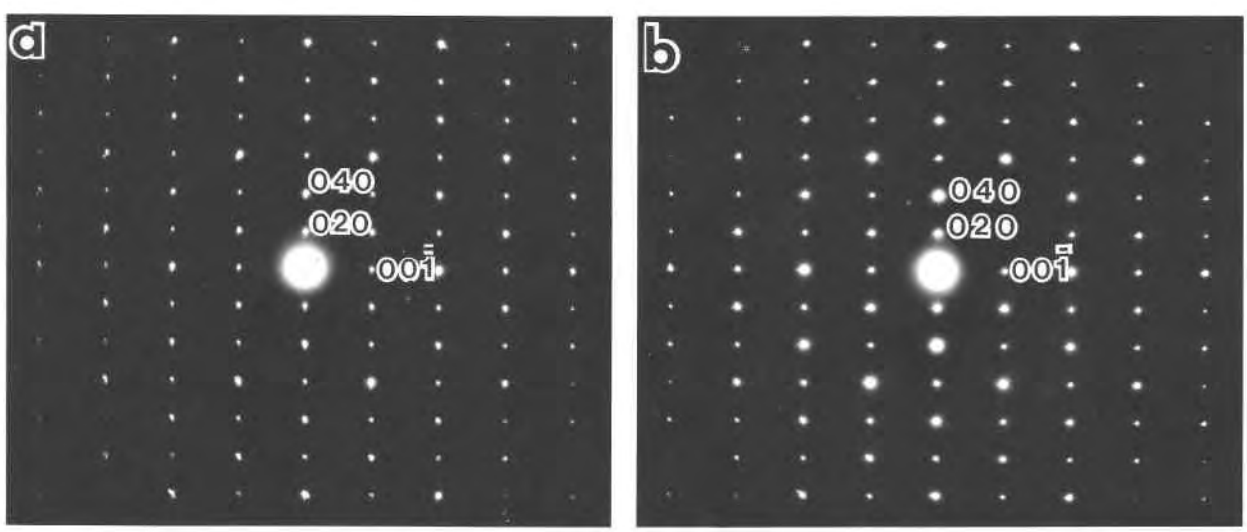

Fig. 3. The [100] electron-diffraction patterns of natural tremolite Tr12 (**a**) and SUMC5122 (**b**).

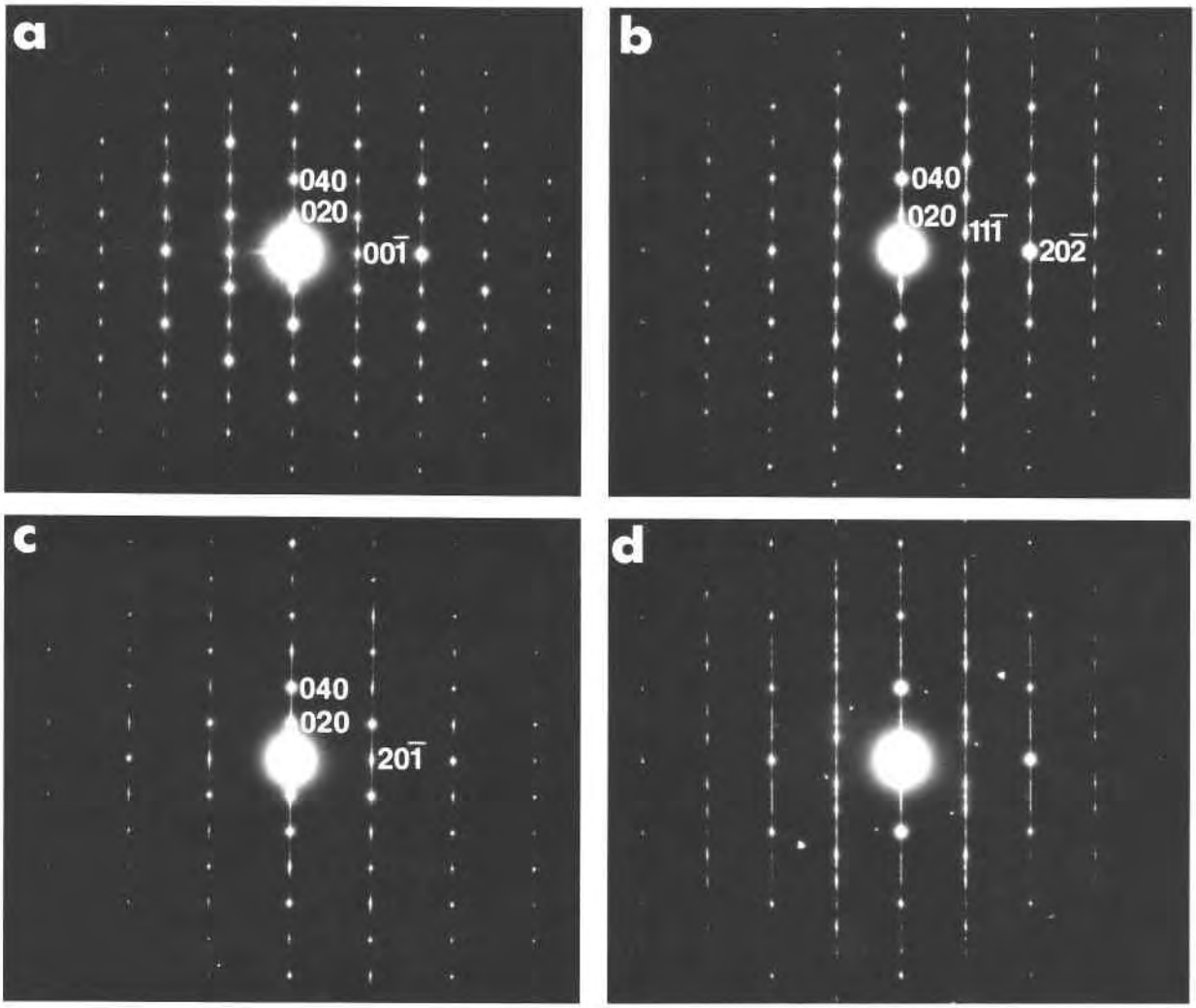

Fig. 4. SAED patterns of synthetic tremolite at (**a**) [100], (**b**) [101], (**c**) [102], and (**d**) [101] orientations. SAED pattern **c** was obtained by rotating the crystal about 24° from the [101] orientation in **b**. SAED pattern **d** is from the highly disordered crystal shown in Figure 7.

firmed by our HRTEM investigation of approximately ten crystals from each tremolite sample.

Electron-diffraction patterns

Because most crystals are elongated along the **c** axis, they settle on the C substrate with their **c** axis approximately perpendicular to the incident electron beam. Therefore, [001] or "I-beam" images were difficult to obtain, and [*h*0*l*] projections were mainly used to examine structural defects. However, since the crystals generally settle on a {110} face, ~28° and ~15° rotations around the **c** and **b** axes, respectively, can achieve the [100] projection.

Two crystal orientations generated most of the microstructural information about chain-width defects for our investigation (Figs. 4a and 4b). The SAED pattern of Figure 4a agrees with the [100] pattern of *C*2/*m* amphibole, but that of Figure 4b is consistent with either a [100] pattern of *Pnma* or a [101] pattern of *C*2/*m* amphibole (Chisholm, 1973). In the [100] pattern of *Pnma* amphibole, 0*kl* reflections with $k + l \neq 2n$ become extinct because of the *n* glide perpendicular to the **a** axis, and the resulting SAED pattern is indistinguishable from a [101] pattern of *C*2/*m* amphibole.

Crystal tilting experiments were performed to check if *Pnma* orthorhombic amphibole coexists with *C*2/*m* monoclinic amphibole. Crystals with **b** axes lying approximately parallel to one of the tilt axes of the TEM stage were selected and rotated around another tilt axis. Depending on the rotation direction, SAED patterns consistent with [100] and [102] orientations were obtained (Fig. 5). Hence, the SAED pattern of Figure 4b corresponds to a [101] pattern of *C*2/*m* rather than a [100] pattern of *Pnma* amphibole. Crystals were rotated from

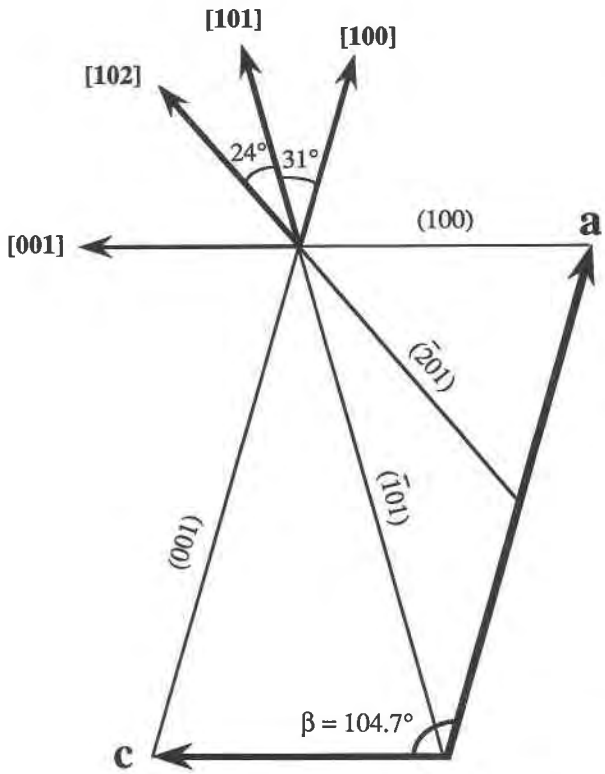

Fig. 5. A projection parallel to the **b** axis of an amphibole crystal onto the (010) plane, showing the relationships among various zone axes and the traces of planes.

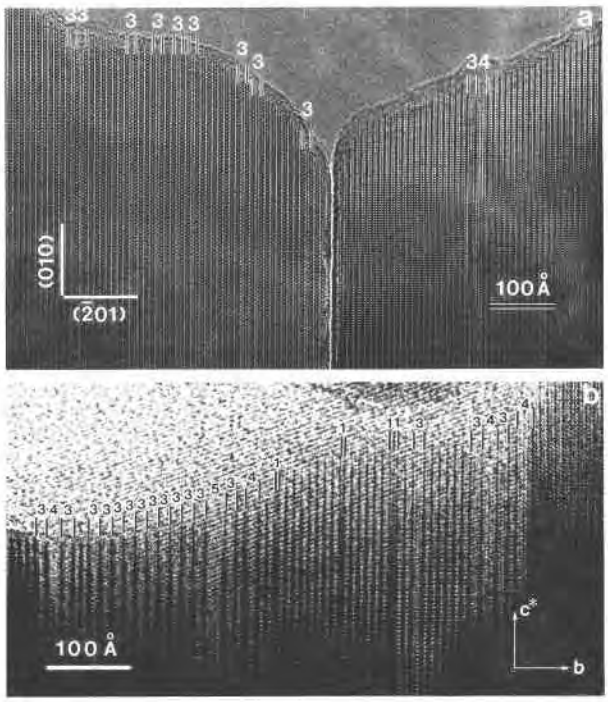

Fig. 6. TEM images of synthetic tremolite containing wide-chain defects. (**a**) Two neighboring crystals in Tr5-18 vary significantly in defect density. The crystal on the left contains more wide-chain slabs (mainly triple-chain structures, labeled 3) than the one on the right. (**b**) A highly disordered crystal containing a slab with ten contiguous triple-chain slabs (Tr1-21). Single-, quadruple-, and quintuple-chain structures (labeled 1, 4, and 5, respectively) are also intergrown.

the [101] orientation by approximately 24° and 31° around the **b** axis to obtain [102] and [100] orientations, respectively.

Most SAED patterns of synthetic amphiboles (Fig. 4) show streaking along the **b*** direction, indicating that chain-width errors are abundant (Veblen and Buseck, 1979; Maresch and Czank, 1983, 1988). In crystals consisting mainly of various wide-chain structures other than double chains, $0k0$ spots with $k \neq 4n$ are heavily streaked (Fig. 4d). Such features result from the perturbation of regular, ordered double-chain periodicities along the **b*** direction caused by the irregular, disordered intergrowth of pyriboles whose chain-widths range from one to six.

Chain-width defects

Double-chain slabs of hydroxyl tremolite and magnesio-hornblende commonly intergrow with other chain-silicate structures (Figs. 6–8). Triple-chain structures predominate among various nondouble chain silicates. They commonly occur in slabs having three to five repeats as well as in isolated single units (Figs. 6 and 7). As many as ten adjacent triple chains were observed in a Tr1-21 crystal (Fig. 6b). Quadruple-, quintuple-, and sextuple-chain structures occur throughout the specimens, but pyribole slabs with chain widths greater than seven were not identified. In Tr2, structurally disordered crystals consisting predominantly of triple chains occur (Fig. 7). Other synthetic amphiboles commonly contain fewer wide-chain structures than those of Tr2. In Figures 6a and 7 the distribution of structural defects varies significantly among individual grains within the same experimental product. A similar observation was made for manganese magnesium amphiboles by Maresch and Czank (1988). These phenomena are attributed to heterogeneous nucleation and growth inside the sample container, as described by Cho and Fawcett (1986) on the basis of size distributions in synthetic crystals of experimental charges.

Single-chain structures in hydroxyl tremolite and magnesio-hornblende occur both as isolated single slabs and as thin packets, producing pyroxene domains ranging up to 0.1 μm in width (Figs. 6b and 8). Pyroxene domains apparently have coherent (101) interfaces with amphiboles.

Virtually no chain-width defects were observed in Tr19-1, in contrast to other synthetic amphiboles; from the 12 crystals examined in detail, only one triple-chain slab was observed. As a result of their more equant habits, some crystals of Tr19-1 settle on the C substrate with their **c** axes subparallel to the incident electron beam. Thus, I-beam images could be obtained with slight tilting.

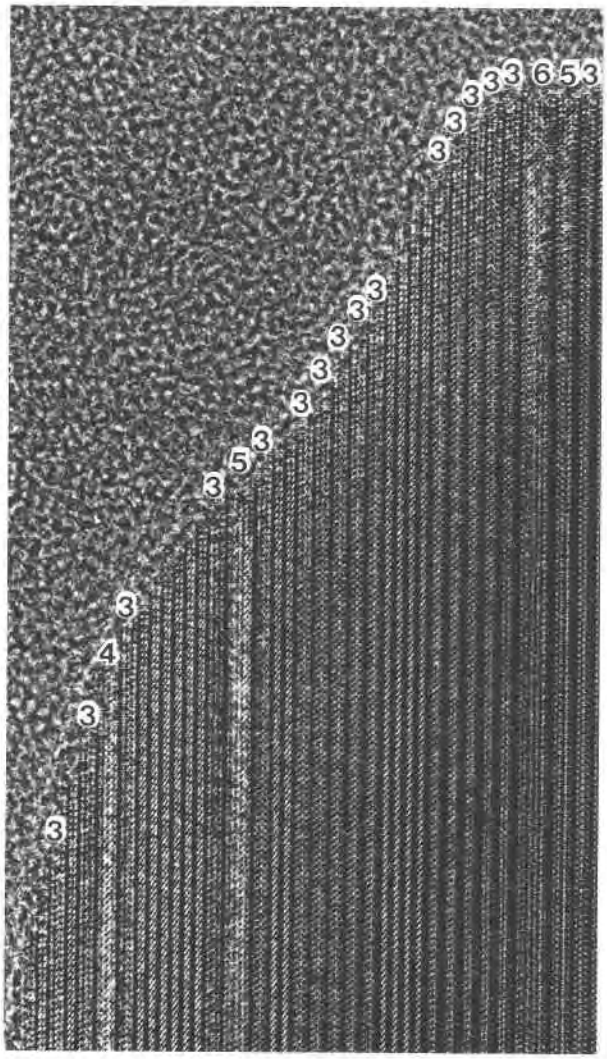

Fig. 7. The (0*k*0) lattice-fringe images from a crystal consisting mainly of triple chains and other wider-chain pyribole structures (Tr2).

The majority of wide- and single-chain structures extend continuously, from end to end of the crystals along the **c** axis, probably as a result of fast growth parallel to the silicate-chain direction. However, cooperative chain terminations (Veblen and Buseck, 1980) occur within some crystals (Fig. 9). The total chain numbers are identical on both sides of the termination, and single-chain structures are typically associated with the terminations. Such terminations may represent either reaction interfaces or growth defects. In the former case, the chain-width defect in Figure 9a can be described by the isochemical solid-solid reaction

$$\underset{m(3)}{Ca_2Mg_8Si_{12}O_{32}(OH)_4} + \underset{m(1)}{Ca_2Mg_2Si_4O_{12}} = 2\underset{m(2)}{Ca_2Mg_5Si_8O_{22}(OH)_2} \quad (1)$$

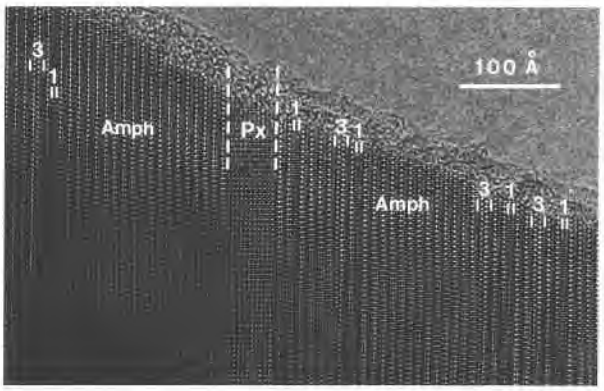

Fig. 8. A thin slab of pyroxene (Px) within a structurally disordered amphibole (Amph) crystal (Tr6). Eleven repeats of single-chain structure occur in the Px slab. Isolated single- and triple-chain slabs also occur.

where m(i) represents the chain-silicate structure with i representing the number of chains in the structure (i = 1 for pyroxenes, 2 for amphiboles, etc.). Hence, one side of the termination contains exclusively double chains, whereas the other side consists of chains having different widths. On the other hand, the chain termination in Figure 9b could result from a reaction of the metasomatic cation-exchange type

$$\underset{m(4)}{Ca_2Mg_{11}Si_{16}O_{42}(OH)_6} + 4Ca^{2+} = 2\underset{m(1)}{Ca_2Mg_2Si_4O_{12}} + \underset{m(2)}{Ca_2Mg_5Si_8O_{22}(OH)_2} + 2Mg^{2+} + 4H^+. \quad (2)$$

The transformation between the two chain sequences observed in Figure 9b requires the diffusion of cations. Furthermore, if wide-chain structures such as m(4) disappear with experiment duration (see below), the formation of m(2)-bearing chain sequences by Reaction 2 necessitates the addition of Ca^{2+} and the concomitant loss of Mg^{2+} and H^+.

A′ values of synthetic amphiboles

To quantify and to compare the amounts of nonamphibole components based on TEM images, Maresch and Czank (1988) defined A and A' values. The A value represents the approximate volume ratio of undisturbed, i.e., greater than unit-cell scale, amphibole components in observed "amphibole" crystals. The A' value is defined as the ratio of the absolute number of double chains—including those occurring in one to three double fringes in the TEM image—to the total number of unit tetrahedral chains in amphibole crystals. Maresch and Czank (1988) further suggested an empirical relationship between A and A' values described by

$$A' \approx A + (1.0 - A)/2.$$

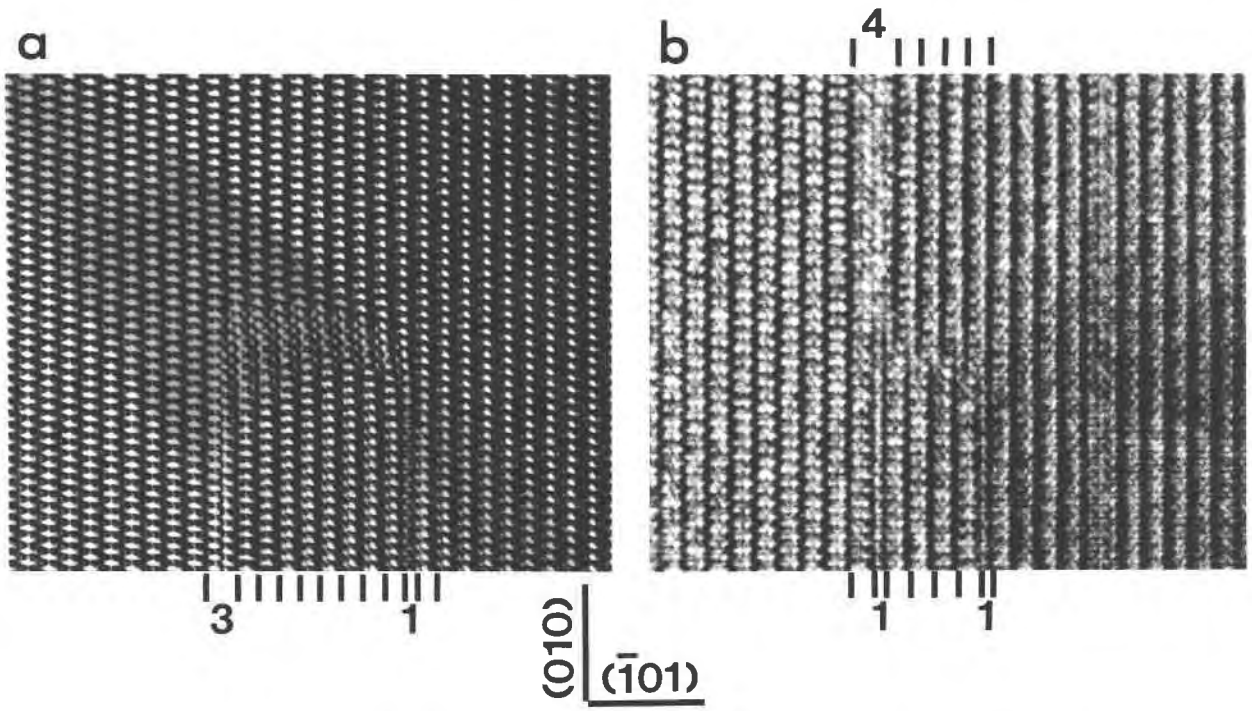

Fig. 9. HRTEM images showing chain-termination defects in synthetic amphiboles. (**a**) Chain terminations of triple- and single-chain slabs (labeled 3 and 1, respectively), resulting in a defect-free region at the top of the image (Tr6). (**b**) The chain sequence (42222) turns into (2122221) along a planar fault (Hb19). A quadruple chain (labeled 4) changes to double- and single-chain slabs; an additional single chain compensates for the chain-width difference.

To examine the relationships among various wide-chain silicate structures, we define $A'(i)$ values for individual pyribole structures as

$A'(i)$ = total width of m(i)/width parallel to **b*** of entire measured crystal

$$= n_i \cdot i \Big/ \sum_i (n_i \cdot i)$$

where n_i denotes the total number of m(i) in the crystal. Thus, the $A'(2)$ value for double-chain silicate of this study is equivalent to the A' value of Maresch and Czank (1988). We find $A'(i)$ values more informative and thus prefer them to A values.

In practice, the $A'(i)$ values can vary from one investigator to another because of different image interpretations, the presence of ambiguous images (Maresch and Czank, 1988), and random sampling error. In our investigation, TEM images were obtained at several different defocus conditions, and those images with the fewest ambiguities were used for counting. More than 20 crystals within each sample were analyzed to obtain the $A'(i)$ values (cf. Maresch and Czank, 1988; Table 2).

The results of our TEM observations are summarized in Table 2 and illustrated in Figure 10. Fluorine tremolite (Tr19-1) yields an $A'(2)$ value of 1.0, whereas the $A'(2)$ values of hydroxyl tremolite range from 0.80 to 0.95. The latter are compatible with the $A'(2)$ values (~0.62–0.95) of manganese magnesium amphiboles reported by Ma-

Table 2. Chain structures and $A'(2)$ values of synthetic amphiboles

Experiment no.	Number of observed crystals	n_1*	n_2	n_3	n_4	n_5	n_6	Number of observed chains	$A'(2)$ value ($\pm 1\sigma$**)	Range in $A'(2)$ values
Tr1-21	20	35	5467	180	23	18	1	5724	0.93 ± 0.07	0.73–0.99
Tr5-18	21	64	2857	208	23	8	2	3162	0.87 ± 0.06	0.78–0.98
Tr2	22	106	2887	363	31	26	5	3418	0.80 ± 0.19	0.28–0.96
Tr6	24	183	5750	107	9	2	1	6052	0.95 ± 0.04	0.83–0.99
Tr19-1	12	0	~2000	1	0	0	0	~2001	1.00	1.00
Hb19	20	77	5096	103	9	2	0	5287	0.96 ± 0.04	0.86–1.00

* Total numbers of individual chain structures. Subscript refers to multiplicity of chain.
** Calculated from the population of $A'(2)$ values of individual crystals examined by HRTEM.

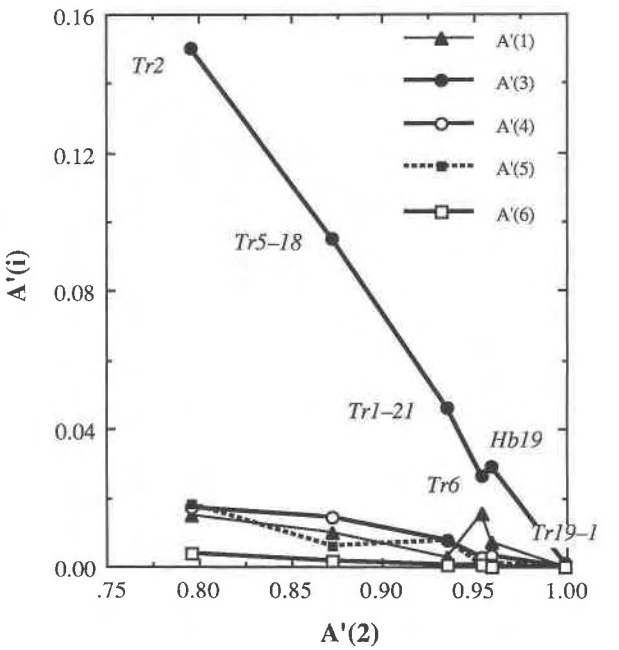

Fig. 10. The A' values of each chain-silicate structure plotted against the $A'(2)$ value. Note that the abundance of triple-chain slabs [$A'(3)$] decreases almost linearly with increasing concentration of double chains in synthetic tremolitic amphiboles.

resch and Czank (1988). The $A'(2)$ value of magnesiohornblende (Hb19) is similar to that of Tr6, which has the highest $A'(2)$ value among hydroxyl tremolite samples. Triple-chain structures predominate among the intergrown pyriboles, and their $A'(3)$ values show a negative correlation with $A'(2)$ values (Fig. 10). The consistent relationship among $A'(i)$ values indicates that the growth mechanism of synthetic amphiboles may not vary significantly as a function of P, T, and compositions. The occurrences of other wide-chain and single-chain structures are relatively minor, and their combined A' values are less than 0.05. Therefore, the inverse relationship between $A'(2)$ and $A'(3)$ values can be generalized as

$$2\ \mathrm{m(3)} + 2\ \mathrm{Ca^{2+}} = 3\ \mathrm{m(2)} + \mathrm{Mg^{2+}} + 2\mathrm{H^{+}}. \quad (3)$$

Discussion

Occurrences of pyriboles

Most chain silicates intergrown with synthetic tremolitic amphiboles occur in disordered sequences, and the repeating units of each pyribole are variable from one to about 100. The ordered sequence of alternating double- and triple-chain structures (clinochesterite structure) was not observed at greater than unit-cell scale. Triple-chain structures are most abundant in Tr2, and their amounts in other specimens decrease systematically with increasing $A'(2)$ values (Fig. 10). Both the predominance of triple-chain structures relative to other wide-chain silicate slabs throughout the specimens and the occurrence of crystals composed mainly of triple chains (Tr2; Fig. 7) suggest the possible presence of a stability field—or at least a local Gibbs free energy minimum—for the triple-chain structure. TEM studies of biopyriboles from Chester, Vermont, also indicated that triple-chain structures may occur as a possible stable phase (Veblen and Burnham, 1978; Veblen and Buseck, 1979; Veblen et al., 1977). In fact, triple-chain sodium magnesium silicates have been synthesized (Drits et al., 1975, 1976; Tateyama et al., 1978), although the existence of stability fields remains to be demonstrated through reversal experiments.

Many single-chain structures are observed from all experimental products except for Tr19-1 (Table 2). Their relative abundance contrasts with the rare occurrence of single chains in synthetic manganese magnesium amphiboles (Maresch and Czank, 1983, 1988). Some isolated single-chain slabs may accompany the crystallization of amphibole slabs, e.g., by Reaction 2. However, thick packets of single chains within an amphibole crystal appear to represent a relict pyroxene precursor reacting to produce amphibole with increasing time. The metastable coexistence of pyroxene and amphibole slabs is shown by double-chain lamellae propagating into the pyroxene slab and by the inverse relation between $A'(2)$ and $A'(1)$ values for hydroxyl tremolite in unseeded experiments (Fig. 10).

Pyribole slabs with chain-widths greater than seven were not observed in any of the products, and talc sheets intergrown with the amphiboles also were not observed. Talc occurs in pseudohexagonal platy crystals in Tr2, but it is absent in products synthesized at higher temperatures. The reaction interface between talc and amphibole was searched for but not found. It is thus likely that talc simply dissolved with increasing temperature and recrystallized as amphibole. Veblen (1981) also indicated that the talc-to-anthophyllite reaction of experimental products is achieved by a dissolution-precipitation mechanism rather than by solid-state recrystallization.

Effect of synthesis variables on structural defects

Temperature appears to be the most critical variable in synthesizing structurally ordered amphiboles. This is most clearly shown by the lack of wide-chain structures in fluorine tremolite (Tr19-1), synthesized at about 1000 °C, as compared to the abundant wide-chain slabs in Tr2, synthesized at 701 °C. Unfortunately, the influence of F on chain-width defects is not known. Temperature also appears to be a more effective control on chain-width disorder than experiment duration. Tr2 was heated for nearly three times as long as Tr1-21 and still has a much lower $A'(2)$ value. This comparison is complicated by a difference in synthesis temperatures of approximately 100 °C but at least indicates that increasing duration by a factor of three cannot compensate for a difference of 100 °C in synthesis temperatures.

The effect of temperature on the concentration of chain-width defects was also reported for manganese magnesium amphiboles by Maresch and Czank (1988). For $Mn_{0.9}Mg_{6.1}Si_8O_{22}(OH)_2$, the $A'(2)$ value at 2 kbar increases

from less than 0.65 at 675 °C to ~0.85 at 750 °C. Maresch and Czank (1988) suggested that amphiboles with few chain-width defects can be synthesized metastably in short-duration experiments at temperatures exceeding those of the amphibole stability field. In order to obtain synthetic tremolite with fewer defects, it may be helpful to synthesize amphiboles at higher temperatures, even metastably beyond their thermal stability limits.

A seeded experimental product, Tr6, shows the highest $A'(2)$ value among hydroxyl tremolite samples, suggesting that the use of stoichiometric nuclei promotes growth of amphibole with relatively few defects. Although some seed crystals may persist as inclusions rimmed by newly grown amphibole, such textures were not identified in Tr6. The seeding technique can greatly facilitate the growth of double-chain silicates by overcoming nucleation barriers. Skogby and Ferrow (1989) synthesized tremolite-actinolite amphiboles that contain structural defects estimated to be less than a few volume percent. They suggested that the incorporation of Ca on the M4 site of the amphibole structure increases the small-scale structural order relative to iron magnesium manganese amphiboles. However, this observation contradicts our results on synthetic calcic amphiboles, which exhibit significant structural defects similar to those in iron magnesium manganese orthoamphiboles. Hence, the high microstructural homogeneity of synthetic calcic amphiboles reported by Skogby and Ferrow (1989) is attributed to their use of 6 wt% natural seed actinolite.

The effect of pressure on the structural defects in synthetic amphibole is difficult to assess because our experiments varied not only in temperature and starting compositions but also in experiment duration. However, even with its short experiment duration, Hb19 synthesized at 10 kbar and 751 °C contains fewer structural defects than the low-pressure hydroxyl tremolite. This observation, in conjunction with the rare occurrence of structural defects in synthetic glaucophane (Koons, 1982), suggests that either high experimental pressure or high Al content enhances the structural order of synthetic amphiboles.

Defect density vs. aspect ratio of crystals

Among the four hydroxyl tremolite samples, Tr2 shows the greatest average aspect ratio. Tr5-18 contains more elongated crystals than Tr1-21, and it has a lower $A'(2)$ value. The sequence of hydroxyl tremolite with increasing $A'(2)$ values (Fig. 10) is consistent with decreasing aspect ratio, Tr2 > Tr5-18 > Tr1-21 ≈ Tr6, i.e., crystal elongation appears to be approximately proportional to the concentration of chain-width errors. Indeed, crystals of Tr19-1 having an $A'(2)$ value of 1.0 are far less elongated than the other products.

Amphiboles break along chains of anomalous width as well as along stacking faults and cleavage planes (Veblen et al., 1977; Veblen, 1980). The former type of break would enhance the elongate morphology of structurally disordered amphiboles. Hence, the aspect ratio of chain-silicate minerals can be related to structural defects as well as to chain mutiplicity; amphiboles containing wide-chain structures generally show more elongate crystal habits than single-chain pyroxenes. The synthetic triple-chain silicate reported by Tateyama et al. (1978) exhibits a far more elongated morphology than that of Tr2 (see their Fig. 2). Such TEM results agree with our observation that aspect ratios are closely related to the structural perfection in synthetic amphiboles. This relationship can also be seen in many TEM investigations of asbestiform amphiboles, which commonly show intergrowths with wide-chain pyriboles (Chisholm, 1973; Hutchison et al., 1975; Veblen et al., 1977; Veblen 1980; Yau et al., 1986; Dorling and Zussman, 1987; Ahn and Buseck, 1991). At least some of the intergrown wide-chain pyriboles in those asbestiform amphiboles were produced by primary growth rather than by alteration processes.

Implications of HRTEM data for the thermal stability of synthetic amphiboles

In addition to structural defects, factors such as f_{H_2O}, grain size, and composition have been suggested as causes for the differences in the thermal stabilities of natural and synthetic tremolite (Jenkins and Clare, 1990). Our HRTEM investigation shows that synthetic tremolite may differ significantly from natural tremolite in defect structure and hence stoichiometry, and widespread disordered intergrowths of single- and wide-chain slabs in synthetic tremolite could be a major cause of contrasting thermal stabilities.

Intergrown wide-chain lamellae cause the bulk composition of synthetic tremolite crystals to deviate from the ideal tremolite composition. Specifically, the wide-chain structures result in a more hydrous composition, and the Ca/Mg ratio is smaller than the ideal value of 0.40. Structure refinement of clinojimthompsonite (Veblen and Burnham, 1978) indicates that in triple-chain structures, Ca is restricted to M5 sites because of its larger cation radius than Mg; amphibole with triple-chain and other wide-chain structures provides fewer crystallographic sites appropriate for Ca than does ideal tremolite. TEM data indicate that the amount of intergrown pyroxene, which can provide more structural sites for Ca, is minor relative to the intergrown wide-chain slabs (Table 2; Fig. 10), and the abundant intergrowth of wide-chain structures contributes to lower Ca/Mg ratios in synthetic crystals. Nonetheless, the abundance of wide-chain defects is insufficient to account for the decidedly low Ca/Mg ratios (0.346–0.356) encountered in the synthetic tremolite (Jenkins, 1987; Graham et al., 1989). For example, synthetic tremolite consisting of 90% double-chain, 9% triple-chain, and 1% quadruple-chain structures results in a Ca/Mg ratio of 0.375, calculated according to the method of Veblen and Buseck (1979) and assuming full occupancy of the outer M sites by Ca (e.g., M4 for amphibole). Although this ratio is lower than that of ideal tremolite (0.40), it is not low enough to match the Ca/Mg ratio observed for synthetic tremolite. For the chain-width percentages mentioned above, a synthetic tremolite

sample must have 5% of the outer M sites occupied by Mg rather than Ca to have a Ca/Mg ratio of 0.356.

Structural defects in minerals are important in controlling diffusion properties and chemical reactions (Buseck and Veblen, 1978; Veblen, 1985). Structural disorder caused by random intergrowths of various chain-silicate structures will increase the Gibbs free energy of synthetic amphiboles relative to defect-free natural ones, at least within the amphibole stability field. Besides the compositional aspect, the structural disorder caused by the intergrowth of various chain widths can play a critical role in modifying thermodynamic properties of synthetic amphiboles.

The extent to which the variation in chain-width defects influences the thermodynamic properties of synthetic tremolite cannot yet be quantified. It is clear from the current study that synthetic tremolite contains a greater percentage of defects than does most natural tremolite. The effects of these chain-width defects on the thermodynamic properties of synthetic tremolite will need to be addressed in future studies of amphibole stability and phase relations.

Conclusions

Chain-width defects are common in synthetic tremolite and hornblende. Triple-chain structures predominate among the defects, the chain widths of which vary from one to six. Single- and triple-chain structures occur in amphibole crystals either as isolated slabs that are one chain wide or as thicker packets. The $A'(2)$ and $A'(3)$ values of synthetic tremolitic amphiboles show a negative correlation, suggesting that the triple-chain silicate is the most important precursor to amphibole.

Temperature is the most important factor governing the presence of chain-width defects in synthetic amphiboles. Crystal habits are correlated with the degree of structural perfection of synthetic tremolite; crystals with a higher aspect ratio tend to contain more abundant chain-width defects. We suggest that the widespread intergrowths of chain-width defects in synthetic tremolite, and the consequent change in composition and degree of structural disorder, explain the apparent lower thermal stability of synthetic tremolite relative to naturally occurring tremolite.

Acknowledgments

Electron microscopy was performed at the Facility for HREM at ASU, which is supported by the NSF and ASU. HRTEM work was supported by NSF grant EAR-8708529 (to P.R.B). Partial support for this study was provided by NSF grants EAR-8803047 (to D.M.J.) and EAR-8616624 (to W.G. Ernst). Invaluable comments and encouragement by W.G. Ernst, as well as helpful and constructive reviews of M. Czank, T.C. McCormick, and D.R. Veblen, are greatly appreciated.

References cited

Ahn, J.H., and Buseck, P. R. (1991) Microstructures and fiber-formation mechanisms of crocidolite asbestos. American Mineralogist, 76, 1467–1478.

Akai, J. (1982) Polymerization process of biopyribole in metasomatism at the Akatani ore deposit, Japan. Contributions to Mineralogy and Petrology, 80, 117–131.

Boyd, F.R. (1959) Hydrothermal investigations of amphiboles. In P.H. Abelson, Ed., Researches in geochemistry, p. 377–396. Wiley, New York.

Buseck, P.R., and Veblen, D.R. (1978) Trace elements, crystal defects and high resolution electron microscopy. Geochimica et Cosmochimica Acta, 42, 669–678.

Chernosky, J.V., Jr., and Autio, L.K. (1979) The stability of anthophyllite in the presence of quartz. American Mineralogist, 64, 294–303.

Chisholm, J.E. (1973) Planar defects in fibrous amphiboles. Journal of Materials Science, 8, 475–483.

Cho, M., and Ernst, W.G. (1991) An experimental determination of calcic amphibole solid solution along the join tremolite-tschermakite. American Mineralogist, 76, 985–1001.

Cho, M., and Fawcett, J.J. (1986) Morphologies and growth mechanisms of synthetic Mg-chlorite and cordierite. American Mineralogist, 71, 78–84.

Dorling, M., and Zussman, J. (1987) Characteristics of asbestiform and non-asbestiform calcic amphiboles. Lithos, 20, 469–489.

Drits, V.A., Goncharov, Y.I., Aleksandrova, V.A., Khadzhi, V.E., and Dmitrik, A.L. (1975) New type of strip silicate. Soviet Physics and Crystallography, 19, 737–741 (translated from Kristallografiya, no. 19, 1186–1193, 1974).

Drits, V.A., Goncharov, Y.I., and Khadzhi, I.P. (1976) Formation conditions and physico-chemical constitution of triple chain silicate with (Si_6O_{16}) radical (in Russian). Izvestiya Akademia Nauk, Seriya Geologiya, 7, 32–41.

Graham, C. M., Maresch, W., Welch, M.D., and Pawley, A.R. (1989) Experimental studies on amphiboles: A review with thermodynamic perspectives. European Journal of Mineralogy, 1, 535–555.

Hutchison, J.L., Irusteta, M.C., and Whittaker, E.J.W. (1975) High resolution electron microscopy and diffraction studies of fibrous amphiboles. Acta Crystallographica, A31, 794–801.

Jenkins, D.M. (1987) Synthesis and characterization of tremolite in the system H_2O-CaO-MgO-SiO_2. American Mineralogist, 72, 707–715.

Jenkins, D.M., and Clare, A.K. (1990) Comparison of the high-temperature and high-pressure stability limits of synthetic and natural tremolite. American Mineralogist, 75, 358–366.

Koons, P.O. (1982) An experimental investigation of the behavior of amphibole in the system Na_2O-MgO-Al_2O_3-SiO_2-H_2O at high pressures. Contributions to Mineralogy and Petrology, 79, 258–267.

Maresch, W.V., and Czank, M. (1983) Phase characterization of synthetic amphiboles on the join $Mn^{2+}{}_xMg_{7-x}[Si_8O_{22}](OH)_2$. American Mineralogist, 68, 744–753.

——— (1988) Crystal chemistry, growth kinetics and phase relationships of structurally disordered (Mn^{2+}, Mg)-amphiboles. Fortschritte der Mineralogie, 66, 69–121.

Skippen, G., and McKinstry, B.W. (1985) Synthetic and natural tremolite in equilibrium with forsterite, enstatite, diopside and fluid. Contributions to Mineralogy and Petrology, 89, 256–262.

Skogby, H., and Ferrow, E. (1989) Iron distribution and structural disorder in synthetic calcic amphiboles studied by Mössbauer spectroscopy and HRTEM. American Mineralogist, 74, 360–366.

Tateyama, H., Shimoda, S., and Sudo, T. (1978) Synthesis and crystal structure of a triple chain silicate, $Na_2Mg_4Si_6O_{16}(OH)_2$. Contributions to Mineralogy and Petrology, 66, 149–156.

Veblen, D.R. (1980) Anthophyllite asbestos: Microstructures, intergrown sheet silicates, and mechanisms of fiber formation. American Mineralogist, 65, 1075–1086.

——— (1981) Non-classical pyriboles and polysomatic reactions in biopyriboles. In Mineralogical Society of America Reviews in Mineralogy, 9A, 189–236.

——— (1985) Extended defects and vacancy non-stoichiometry in rock-forming minerals. In R.N. Shock, Ed., Point defects in minerals, p. 122–131. American Geophysical Union, Washington, DC.

Veblen, D.R., and Burnham, C.W. (1978) New biopyriboles from Chester, Vermont: II. The crystal chemistry of jimthompsonite, clinojimthompsonite, and chesterite, and the amphibole-mica reaction. American Mineralogist, 63, 1053–1073.

Veblen, D.R., and Buseck, P.R. (1979) Chain-width order and disorder in biopyriboles. American Mineralogist, 64, 687–700.

——— (1980) Microstructures and reaction mechanisms in biopyriboles. American Mineralogist, 65, 599–623.

Veblen, D.R., Buseck, P.R., and Burnham, C.W. (1977) Asbestiform chain silicates: New minerals and structural groups. Science, 198, 359–365.

Yau, Y.-C., Peacor, D.R., and Essene, E.J. (1986) Occurrence of wide-chain Ca-pyriboles as primary crystals in the Salton Sea Geothermal Field, California, USA. Contributions to Mineralogy and Petrology, 94, 127–134.

Manuscript received September 10, 1990
Manuscript accepted June 30, 1991